# Cable bacteria colonise new sediment environments through water column dispersal

van Dijk, Jesper R.; Geelhoed, Jeanine S.; Ley, Philip; Hidalgo-Martinez, Silvia; Portillo-Estrada, Miguel; Verbruggen, Erik; Meysman, Filip J.R.

**DOI**
10.1111/1462-2920.16694

**Publication date**
2024

**Document Version**
Final published version

**Published in**
Environmental Microbiology

**Citation (APA)**
van Dijk, J. R., Geelhoed, J. S., Ley, P., Hidalgo-Martinez, S., Portillo-Estrada, M., Verbruggen, E., & Meysman, F. J. R. (2024). Cable bacteria colonise new sediment environments through water column dispersal. *Environmental Microbiology*, *26*(10), Article e16694. https://doi.org/10.1111/1462-2920.16694

Received: 13 March 2024 | Accepted: 15 August 2024

DOI: 10.1111/1462-2920.16694

RESEARCH ARTICLE

ENVIRONMENTAL MICROBIOLOGY

# Cable bacteria colonise new sediment environments through water column dispersal

**Jesper R. van Dijk**[1] | **Jeanine S. Geelhoed**[1] | **Philip Ley**[1] | **Silvia Hidalgo-Martinez**[1] | **Miguel Portillo-Estrada**[2] | **Erik Verbruggen**[2] | **Filip J. R. Meysman**[1,3]

[1]Research group Geobiology, Department of Biology, University of Antwerp, Antwerp, Belgium

[2]Research group Plants and Ecosystems, Department of Biology, University of Antwerp, Antwerp, Belgium

[3]Department of Biotechnology, Delft University of Technology, Delft, The Netherlands

**Correspondence**
Filip J. R. Meysman, Department of Biology, University of Antwerp, 2610 Wilrijk, Antwerp, Belgium.
Email: filip.meysman@uantwerpen.be

**Funding information**
Fonds Wetenschappelijk Onderzoek, Grant/Award Number: S004523N; Universiteit Antwerpen; HORIZON EUROPE European Innovation Council, Grant/Award Number: 101046719

**Abstract**

Cable bacteria exhibit a unique metabolism involving long-distance electron transport, significantly impacting elemental cycling in various sediments. These long filamentous bacteria are distributed circumglobally, suggesting an effective mode of dispersal. However, oxygen strongly inhibits their activity, posing a challenge to their dispersal through the water column. We investigated the effective dispersal of marine cable bacteria in a compartmentalised microcosm experiment. Cable bacteria were grown in natural 'source' sediment, and their metabolic activity was recorded in autoclaved 'destination' cores, which were only accessible through oxygenated seawater. Colonisation occurred over weeks, and destination cores contained only one cable bacterium strain. Filament 'snippets' (fragments with a median size of ~15 cells) accumulated in the microcosm water, with about 30% of snippets attached to sediment particles. Snippet release was also observed in situ in a salt marsh creek. This provides a model for the dispersal of cable bacteria through oxygenated water: snippets are formed by filament breakage in the sediment, released into the overlying water and transported with sediment particles that likely offer protection. These insights are informative for broader theories on microbial community assembly and prokaryotic biogeography in marine sediments.

## INTRODUCTION

Cable bacteria are long, filamentous bacteria that inhabit both marine and freshwater sediments (Malkin et al., 2014; Pfeffer et al., 2012; Risgaard-Petersen et al., 2015). They perform electrogenic sulphur oxidation (e-SOx), in which the oxidation of sulphide in deeper sediment layers is electrically coupled to the reduction of oxygen near the sediment–water interface (Meysman et al., 2019; Nielsen et al., 2010). The required long-range electron transport occurs through a network of conductive fibres that span the length of the filament (Meysman et al., 2019). Previous studies have provided insight into the geographical distribution and diversity of cable bacteria in natural sediment environments (Dam et al., 2021; Geelhoed et al., 2023; Marzocchi et al., 2014; Marzocchi et al., 2018; Scholz et al., 2021; Trojan et al., 2016). While the community assembly of cable bacteria has not been systematically studied, there seems to be a pattern emerging: sediment from one location can harbour multiple strains of cable bacteria, while conversely, the same species can be found within coastal sites on different continents. For example, the marine species *Ca.* Electrothrix communis has been detected in sediments on both sides of the North Atlantic (Trojan et al., 2016), while the large cell-sized marine cable bacterium *Ca.* Electrothrix gigas has been found in dense numbers at several sites in

NW Europe and Australia (Geelhoed et al., 2023). In a similar fashion, a single sediment has been demonstrated to host multiple cable bacterium species with different morphology (Geelhoed et al., 2023; Marzocchi et al., 2018), thus raising questions about niche differentiation within electrogenic sulphur oxidation and the cable bacterium clade. As such, cable bacteria seem to illustrate the Baas Becking tenet 'Everything is everywhere, but the environment selects' (Becking, 1934; de Wit & Bouvier, 2006). This hypothesis has been the starting point for many studies of microbial biodiversity and their biogeographical patterns, fuelling the debate regarding to what extent microorganisms are truly cosmopolitan (Cho & Tiedje, 2000; Fenchel & Finlay, 2004; Staley & Gosink, 1999).

In essence, the Baas Becking (1934) hypothesis implies that microorganisms are not subject to dispersal limitation. However, studies performed in the last ~25 years have accumulated evidence that microorganisms are restricted in their dispersal. Spatial patterns of microbial community diversity show a decrease in composition similarity with larger geographic distances. Similarly, the genetic differentiation of microbial populations increases with a larger spatial scale. Microcosm experiments have shown the impact of dispersal on microbial evolution, community assembly and functioning (see Barbour et al., 2023, Hanson et al., 2012 and references therein). While 'dispersal' is generally defined as the movement of organisms across space and time (Vellend, 2010), the ability to colonise new places is termed 'effective dispersal' (Custer et al., 2022). Dispersal can be categorised into two mechanisms: active and passive. Active dispersal involves direct movement through internal processes (e.g., flagellar movement), while passive dispersal is driven by external forces, such as water currents (Custer et al., 2022). For microorganisms inhabiting marine sediments, effective dispersal requires that they can move across long distances (~10–1000 km), but also that they can suitably survive this journey and establish a new population. This ensures continuous colonisation of spatially segregated sediments and provides a homogeneous distribution across different oceanic environments.

At present, the mechanism of effective dispersal of cable bacteria remains enigmatic. In essence, there are two possible migration routes: either through the sediment or via the water column. Lateral transfer through the sediment is possible, as cable bacteria are known to possess gliding motility, enabling velocities up to 1 $\mu m\ s^{-1}$ (Bjerg et al., 2016; Geelhoed et al., 2023) and lateral spreading rates up to 1.2 $cm\ day^{-1}$ have been recorded (Yin et al., 2021). However, lateral migration through the sediment comprises a very slow distribution mechanism, which does not appear fast and effective enough to ensure dispersal across regional and continental scales. For example, regional spreading across the North Sea (distance ~100 km) would require a minimum of 30,000 years, while intercontinental spreading along shorelines (~40,000 km) would require at least 10 million years. Likewise, bacteria would need to traverse unsuitable habitats (e.g., rocky shores or gravel beds). Therefore, lateral transfer of cable bacteria likely occurs through the water column, which enables a far more rapid form of dispersal. As it happens, dispersal through the water column was hypothesised to occur (but not systematically investigated) in a previous laboratory incubation study (Geelhoed et al., 2020). The development and growth of cable bacteria in sediment cores was observed to be accelerated by the presence of nearby cores in the same microcosm with already active cable bacteria (Geelhoed et al., 2020).

Dispersal through the water column also poses a critical challenge for cable bacteria, since coastal waters typically have high concentrations of dissolved oxygen. While cable bacteria do use $O_2$ as an electron acceptor, they do not seem to tolerate high $O_2$ levels. Cable bacteria inhabit mostly the anoxic part of the sediment, share a common ancestry with strictly anaerobic sulphate reducers, and their genome makeup includes many anaerobic metabolic pathways (Kjeldsen et al., 2019). Their micro-aerophilic nature is aptly illustrated by microcosms studies, where cable bacteria migrate out of anoxic sediment towards oxygen, but stop their journey within the microaerophilic zone (<10 $\mu M\ O_2$) and do not further venture into zones with higher oxygen levels (Bjerg et al., 2023; Scilipoti et al., 2021). Moreover, it has been shown that exposure to air results in a rapid decrease (>90% within 15 min) of the conductance of cable bacterium filaments, while conductance remains stable under an $N_2$ atmosphere or vacuum (Meysman et al., 2019; van der Veen et al., 2024). This suggests that the viability of cable bacterium filaments could be strongly impaired when transported through oxygenated water, and so the question remains as to how cable bacteria can attain 'effective dispersal' in aquatic environments.

Insight into the mechanisms of community assembly in filamentous cable bacteria could be informative for broader theories on prokaryotic biodiversity and their biogeographical patterns. Cable bacteria provide a good case study, as within the microbial realm, they show several features that could limit effective dispersal: (1) their filamentous nature likely slows down dispersal compared to unicellular microorganisms, (2) they reside in the sediment, which implies a barrier to transport as compared to water column microorganisms (i.e., they need to exit the sediment) and (3) they adhere to an anoxic lifestyle, which likely hampers their survival during the transit in an oxygenated water column. To verify if and how cable bacteria are capable of water column dispersal and subsequent sediment colonisation, we performed a dedicated microcosm experiment, in which the microcosm was divided into two

segregated sections: one with natural sediment containing cable bacteria (the 'source') and another with autoclaved sediment cores (the 'destination'). The only physical connection between these compartments is the overlying, aerated seawater. To demonstrate colonisation of new sediments, we employed microsensor profiling to verify the metabolic activity of cable bacteria, combined with 16S rRNA gene amplicon sequencing to examine the diversity of cable bacteria. Additionally, we determined whether cable bacteria were present in the overlying water. To link our lab experiment results with the natural environment, we also performed a field investigation of a creek bed within a salt marsh.

## EXPERIMENTAL PROCEDURES

### Field site and sediment collection

Sediment for the microcosm experiment was collected in June 2022 from a salt marsh (Rattekaai, The Netherlands; 51.439051° N, 4.168504° E) where previously cable bacteria have been found in situ (Malkin et al., 2014). To this end, the top 15 cm of the sediment was collected at low tide from the creek bed and stored in a dark box with overlying water at room temperature until further use. The same site was revisited in February 2023 at low tide to conduct in situ observations. At the time of sampling, the creek was largely drained and the creek bed was covered by a shallow, stagnant layer of overlying water (~20 mm height). This overlying water was collected with a 50 mL syringe connected to a 4 mm inner diameter tubing without disturbing the sediment to examine the presence of cable bacteria. Subsequently, six in situ sediment cores (polycarbonate core liners, inner diameter 40 mm) were taken, close to where overlying water was sampled. Sediment cores were transported back to the lab for microsensor profiling to verify the metabolic activity of cable bacteria. The bulk sediment sampled in June 2022 was analysed for grain size by Mastersizer 2000, Malvern Panalytical. The solid phase density (g $cm^3$),

$$\rho_{sed} = M_{sed}/V_{dis},$$

is measured by adding a known mass $M$ of dry sediment (g) to a graduated cylinder filled, while the subsequent volume displacement $V_{dis}$ ($cm^3$) is recorded. Sediment porosity,

$$\varphi_{sed} = V_{por}/V_{sed},$$

was determined from water content and solid phase density measurements, accounting for the salt content of the pore water.

Water content was determined as the volume of water removed by freeze-drying (Christ Freeze Dryer ALPHA 1-2 LDplus, Osterode am Harz, Germany) wet sediment samples to a constant weight. Total organic and inorganic carbon and C:N ratio were measured with the Dumas dry combustion method (model Flash 2000 NC Soil Analyser, Interscience, Louvain-la-Neuve, Belgium). Elemental analysis was measured using 7700x ICP-MS on samples digested with aqua regia (Agilent Technologies, Inc., Santa Clara, CA, United States).

### Laboratory incubation experiment

The sediment collected was sieved (<1.4 mm) to remove invertebrates, shells and rocks. Part of the sieved sediment was used as such ('natural sediment') to act as source sediment, while another part was autoclaved for 25 min at 121°C ('autoclaved sediment'). A microcosm (23 × 16 × 16 cm, w × d × h) was divided into two parts by placing a separator with a height of 11 cm (Figure 1). One part of the microcosm was filled with natural sediment (1.6 L or ~10 cm height). This compartment was intended to induce rapid cable bacterium growth, and hence functioned as the source for cable bacterium dispersal, further referred to as 'natural sediment' treatment (or 'NS'). The other part of the microcosm was filled with seawater, into which six separate cores with autoclaved sediment were placed. To this end, four polycarbonate cylinders (10 cm high and 4.0 cm inner diameter, closed at the bottom with a rubber stopper) were filled with autoclaved sediment, while two other cylinders (10 cm high and 2.8 cm inner diameter, closed at the bottom with a rubber stopper) were similarly filled but additionally covered with a polycarbonate membrane filter (GTTP, pore size 0.22 μm, Merck Isopore, Germany) secured to the wall of the core with parafilm. The four sediment cores functioned as potential destination sites for effective dispersal (henceforth referred to as 'destination cores' or 'DC'), while the two covered cores had a physical barrier that should prevent inoculation of cable bacteria (referred to as 'negative controls' or 'NC'). After leaving the sediment to settle for ~20 h, the microcosm was placed inside a larger container (40 × 30 × 20 cm), and the setup was filled with artificial seawater with salinity 32 (ASW; Instant Ocean Sea Salt, total volume 18 L) to ensure overlying water. The larger container ensured a 'water connection' between the two compartments of the microcosm and allowed water oxygenation without sediment disturbance. Approximately 4 cm of overlying water was present over the natural sediment and the six sediment cores. The microcosm was kept at 19°C in the dark and was not moved during the timespan of the experiment. Two small aquarium pumps (on either side of the microcosm) kept the water oxygenated through bubbling. This maintained a gentle water flow in the

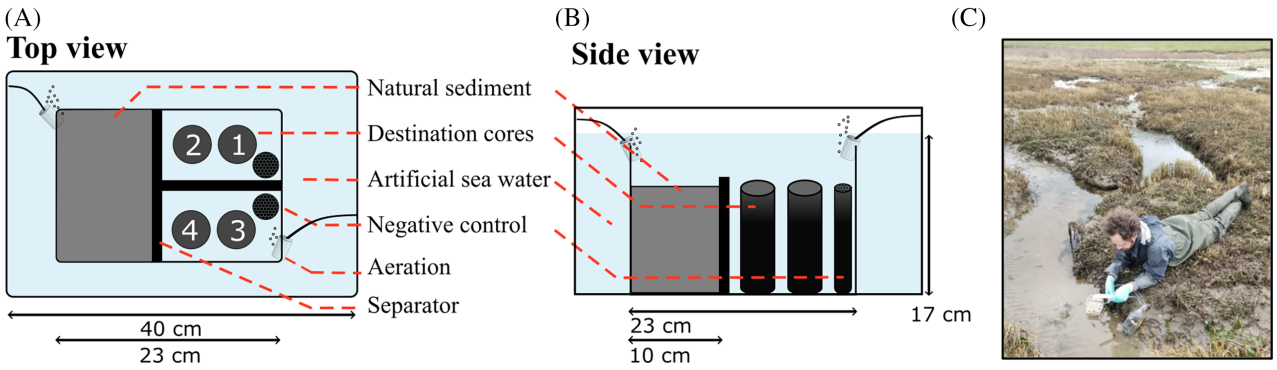


**FIGURE 1** Microcosm dispersal experiment: (A) top view and (B) side view. A microcosm was split into two halves separated by a 0.5-cm-thick plastic separator. One side contained natural sediment as a source for cable bacterium dispersal. The other side contained 4 'destination cores' with autoclaved sediment to be colonised. Two additional cores were also filled with autoclaved sediment but shielded from colonisation by a membrane (negative controls). The only physical connection was the overlying water, which was oxygenated with aquarium pumps. (C) Salt marsh location used for sediment collection and field investigation. At low tide, the sediment in the creek bed was covered by a stagnant layer of overlying water. Sediment cores were taken, and overlying water was sampled.

mesocosm, which minimises disturbance of the sediment while keeping the overlying water sufficiently in circulation. The water was not replaced during the experiment to allow the detection of filaments that possibly accumulated in the overlying water.

## Microsensor depth profiling

The metabolism of cable bacteria imposes a characteristic fingerprint upon the pore water of the sediment (Meysman et al., 2015; Nielsen et al., 2010), which can be evaluated by microsensor depth profiling of pore water solutes ($O_2$, $H_2S$, pH) and electrical potential (EP). To track the temporal development of cable bacteria activity in the natural sediment and destination cores, we recorded depth profiles (down to 3.0 cm). To this end, we used commercial micro-electrodes (Unisense A.S., Denmark) for dissolved $H_2S$ (100 μm tip diameter), $O_2$ (50 μm tip), pH (200 μm tip) and EP (100 μm tip), a Multimeter amplifier system (Unisense A.S., Denmark) and a motorised micromanipulator (Unisense A.S., Denmark). Depth profiles were recorded in duplicate for the natural sediment and each destination core. Microsensor calibration was performed as in Malkin et al. (2014): $O_2$ electrodes were calibrated using a two-point calibration made in air-saturated seawater (100%) and the anoxic zone of the sediment (0%); $H_2S$ microsensors were calibrated using $Na_2S$ standards in anoxic acidified ASW (pH 3.5) within the range of 0–50 μM; for pH, three NBS standards (pH 4, 7 and 10) were used to calibrate the sensor. The oxygen penetration depth (OPD) was determined as the depth with $O_2$ concentrations <1 μM. Total sulphide ($\Sigma H_2S$) was calculated based on the dissolved $H_2S$ concentration and pH with apparent $pK_a$ values for $H_2S$. The sulphide appearance depth (SAD) was set as the depth where $H_2S$ concentrations first exceeded >20 μM. The depth of the suboxic zone was determined as $\Delta L = \text{SAD} - \text{OPD}$. ΔpH was determined as the difference between the pH value at the deepest point (30 mm) and the minimum pH value recorded in the sediment ($\Delta pH > 0$ hence indicating a subsurface minimum). Finally, the EP signal was measured as described by Damgaard et al. (2014). ΔEP was calculated as the difference between the values at the sediment–water interface and the deepest point (30 mm).

## Sampling of sediment and overlying water

Both natural sediment and destination cores were micro-profiled at regular two-week intervals. Sediment samples from the natural sediment treatment were taken for fluorescent in situ hybridisation (FISH) and DNA analysis at 0, 54 and 85 days. To not disturb the sediment as the incubation continued, a small scoop of sediment was carefully collected from the top 4 mm (with a surface area of ~0.5 $cm^2$). In a destination core, sediment for FISH and DNA analysis was collected after the characteristic fingerprint of cable bacteria metabolism was detected (increased ΔpH and/or ΔEP). To this end, the core was taken from the microcosm set-up, and sectioned, collecting the 2–6 mm depth layer of sediment (which was assumed to contain the largest density of cable bacteria). On the same day, a negative control core was sampled at 2–6 mm. The sediment samples were individually homogenised, after which a subsample was immediately frozen in liquid nitrogen and stored at −80°C for DNA extraction, and another subsample was fixed in 96% ethanol (1:1 w/v) and stored at −20°C for FISH. Overlying water samples were collected biweekly with a 50 mL syringe and filtered using a polycarbonate membrane filter (0.22 μm) placed on a support filter (0.45 μm mixed cellulose ester, Whatman 10401606, Merck Isopore, Germany)

with a Sartorius filtration unit. A volume of 50 mL was filtered for FISH and 200 mL for DNA extraction.

## Microbial community analysis

DNA was extracted, either from ~0.4 g sediment or, in the case of the overlying water, the 0.22 μm filters cut into small pieces, using the DNeasy PowerSoil Pro kit (QIAGEN). The V3–V4 16S rRNA region was amplified using 341F and 785R primers (Herlemann et al., 2011) with added Illumina adapters using Phusion polymerase (New England Biolabs) and ~ 1 ng/μL template. The cycling parameters were: initial denaturation at 98°C for 1 min, followed by 27 cycles of denaturation at 98°C for 30 s, annealing at 57°C for 30 s and extension at 72°C for 30 s. The final extension was performed at 72°C for 5 min. Amplified DNA was checked for size on the gel, and excess primers and dNTPs were removed using Exo-CIP (New England BioLabs). Library preparation and MiSeq sequencing (2 × 300 bp) were performed at Eurofins Genomics, Constance, Germany.

Sequences were processed and amplicon sequence variants (ASVs) were analysed using the dada2 pipeline (Callahan et al., 2016). Optimal size trimming positions were obtained using Figaro (Sasada et al., 2020). ASVs that had ≥10 accumulative counts and were present in ≥2 samples were retained and classified against the Silva small subunit rRNA database v138 (Quast et al., 2013). This was done to filter out low-abundance sequences that might be erroneous or noisy (Duvallet et al., 2017; Nikodemova et al., 2023). The detection limit per sample was calculated as 10 divided by the total number of counts/sample. The α-diversity was evaluated for each sample (rarefied to the lowest total number of counts/sample) using the number of observed ASVs and Shannon index with the *microbiome* (v1.20.0) package in Rstudio (Lahti & Shetty, 2012–2019). The classified taxa were aggregated at the genus level, and the ordination pattern of samples was determined by non-metric multidimensional scaling (NMDS) using the Bray–Curtis dissimilarity index, on compositional data, as implemented using MicroViz (Barnett et al., 2021). Further processing and visualisation were done using the *phyloseq* (McMurdie & Holmes, 2013) and *vegan* (v2.6-4) packages.

## Fluorescence in situ hybridisation

FISH was used to assess the abundance of cable bacteria in the natural sediment, the destination cores, negative controls and the overlying water. For the sediment samples, 100 μL of ethanol-fixed sediment was transferred to 500 μL of a 1:1 mixture of ASW and ethanol, and 10 μL of this mixture was filtered over a polycarbonate membrane filter (type GTTP, pore size 0.22 μm, Merck Isopore, Germany). In the case of the overlying water, 50 mL was filtered and fixed in 2 mL of 1:1 AWS:ethanol for 30 min. Filters were subsequently washed with milliQ water, embedded in 0.1% low-melting point agarose and stored at −20°C until further use. FISH was performed on filter pieces according to previously published protocols (Pernthaler et al., 2001; Schauer et al., 2014) with probes DSB706, targeting the *Desulfobulbaceae* (Loy et al. 2002, Lücker et al. 2007), EUB338 as positive control and NON338 as negative control. Hybridised filters were mounted on a microscopy slide and counterstained with 2 μg/mL 4′,6-diamidino-2-phenylindole (DAPI) in 8:2 Citifluor/Vectashield.

Hybridisation was evaluated using a Zeiss Axioplan 2 epifluorescence microscope. Images were taken with a Qimaging EXi Blue camera, and image processing was performed with Image-Pro Insight (Media Cybernetics, U.S.A.) and ImageJ software (Schindelin et al., 2012). To quantify the cable bacteria filament length in a sample, 200 unique fields (105 × 141 μm) were analysed. Instead of individual cell counts, the volumetric filament density $\rho_{vol}$ (m of filament per $cm^3$ of wet sediment or per $cm^3$ of overlying water) was quantified as a measure of cable bacterium abundance. If a hybridised filament was present in a given field, its length and diameter were recorded. The observed length values in the 200 fields were summed and recalculated to the associated volumetric filament density (accounting for the volume of wet sediment or filtered overlying water that was analysed). The areal filament density in the sediment $\rho_{area,sed}$ (m of filament per $cm^2$) was calculated as

$$\rho_{area,sed} = \rho_{vol,sed} \times SAD.$$

As shown previously, the extent of the suboxic zone closely approximates the depth where cable bacteria are abundantly present (Geelhoed et al., 2020; Schauer et al., 2014). The areal filament density was multiplied by the core surface area to calculate the total filament length within the core,

$$\rho_{core} = \rho_{area,sed} \times A_{sed\_core}.$$

The areal filament density in the water column (m of filament per $cm^2$ of natural sediment, length of filaments when projecting downwards over a 1 cm × 1 cm area of sediment) was calculated as

$$\rho_{area,wat} = \rho_{vol,wat} \times V_{wat}/A_{sed},$$

where $V_{wat} = 18{,}000\ cm^3$ is the water volume in the setup and $A_{sed} = 160\ cm^2$ is the surface area of the natural sediment, which acts as a source for the filaments in the overlying water. The net cell release rate from the sediment (cable bacteria cells $m^{-2}\ h^{-1}$) was calculated as

$$R_{\text{cell}} = \left(\rho_{\text{area,wat}}\left(t+\Delta t\right) - \rho_{\text{area,wat}}(t)\right)/\left(L_{\text{cell}} \times \Delta t\right),$$

where the average cell length $L_{\text{cell}} = 3.3$ μm was determined from FISH analysis and $\Delta t$ is the period between two consecutive time points. For the filament fragments of cable bacteria present in the overlying water, further referred to as 'snippets', the median snippet length was calculated based on all snippets present in the 200 analysed fields. The average of this median was calculated across all time points to arrive at the 'overall median snippet length', which was employed to estimate the time of effective dispersal in the destination cores (see below). The detection limit of our FISH method for cable bacteria in the sediment was calculated to be 1 m $cm^{-3}$. In the case of the overlying water, the detection limit was 1 filament $cm^{-3}$ overlying water.

## RESULTS

### Sediment characteristics

The sediment was cohesive and had a median grain size of 54 μm (measured by Mastersizer 2000, Malvern Panalytical), a solid phase density of 2.44 g $cm^{-3}$ sediment and a porosity of 0.92. Additionally, the sediment had a total organic carbon content of 1.8% and total inorganic carbon content of 1.7% (dry sediment weight), and a molar total organic carbon to total nitrogen ratio (C:N) of 11.7 based on the Dumas dry combustion method. Elemental analysis revealed Ca, Fe, Mg, Mn, P and S contents of 12.2, 7.1, 3.8, 0.1, 0.4 and 4.9 mg $g^{-1}$ dry sediment, respectively, measured using 7700x ICP-MS on samples digested with aqua regia (Agilent Technologies, Inc., Santa Clara, CA, United States).

### Development of cable bacteria in the natural sediment

Specific changes in the pore water geochemistry, as documented by microsensor depth profiling, can be used as a reliable indicator of the metabolic activity of cable bacteria (Meysman et al., 2015; Nielsen et al., 2010). As known from previous incubation studies (Burdorf et al., 2017; Schauer et al., 2014), three specific parameters are indicative of the intensity of e-SOx activity: (1) the formation of a subsurface pH minimum (as quantified by a positive excursion of ΔpH), (2) the formation of a suboxic zone $\Delta L > 0$ and (3) the build-up of an electrical potential signal (ΔEP >0), which forms a direct indication that long-distance electron transport rate is taking place (Damgaard et al., 2014). Figure 2 shows the evolution of these three e-SOx indicators (ΔpH, ΔL and ΔEP) throughout the incubation experiment. The underlying microsensor depth profiles are given in Figure A1.

At the start of the incubation, the natural sediment treatment showed no subsurface pH maximum ($\Delta pH = 0$), no electrical potential signal and no suboxic zone: oxygen was depleted below 1 mm and sulphide levels increased directly below the oxygen penetration depth (Figures A1 and A2). Yet, after 14 days of incubation, the characteristic geochemical fingerprint of cable bacteria became noticeable: a pH minimum emerged at 7 mm depth ($\Delta pH = 1.2$), a suboxic zone developed ($\Delta L = 4$ mm) and an increase in EP ($\Delta EP = 0.6$ mV) was recorded over the depth of the suboxic zone (Figure 2). By Day 28, cable bacteria had grown deeper into the natural sediment, as indicated by the subsurface pH minimum at 13 mm depth. The suboxic zone increased ($\Delta L = 8$ mm), and the sulphide concentration remained relatively low beyond the suboxic zone down to 17 mm, the depth where the largest ΔEP (0.7 mV) was reached. Subsequently, cable bacteria activity appeared to wane (Figure 2), consistent with the boom–bust cycle that has been observed previously in other incubations of natural sediments (Burdorf et al., 2018; Schauer et al., 2014). By Day 54, all indicators of cable bacteria had decreased ($\Delta L = 5$ mm, ΔpH and ΔEP vanished in one of the two profiled sediment spots), while at 75 days, there appeared again a small surge in activity (Figure 2). The abundance of cable bacteria as determined by FISH was in line with the e-SOx activity as recorded by microsensor depth profiling. At the start of the experiment, the natural sediment showed a low filament density of 6 m $cm^{-3}$. The filament density increased markedly to 107 m $cm^{-3}$ after 54 days and was again lower at the end of the experiment (45 m $cm^{-3}$ after 85 days). Filament diameters in the natural sediment varied from 0.4–1.6 μm with a median of 0.9 μm and did not show any temporal trend. The mean cell length was 3.3 ± 0.5 μm.

### Development of cable bacteria in the destination cores

At the start of the experiment, the destination cores (DC1 to DC4) showed no free sulphide, which likely resulted from the sediment autoclaving (Figure A1). Yet, after 14 days of incubation, free sulphide concentrations had accumulated to similar levels of the natural sediment. For some time, the destination cores showed similar microsensor depth profiles, resembling those of the natural sediment at Day 0 (i.e., with no indication of cable bacterium activity; Figures A1 and A2). This period lasted for a different time in each core (Figure 2). After 54 days, the metabolic fingerprint of cable bacteria was detected in a first destination core (DC1), showing a subsurface pH

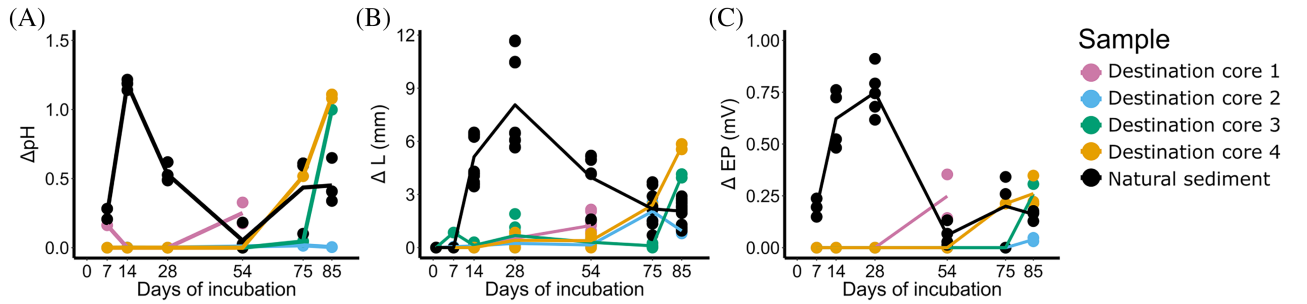


**FIGURE 2** Temporal evolution of three indicators of metabolic activity of cable bacteria throughout the experiment (natural sediment and destination cores). (A) The pH excursion ΔpH. (B) The extent of the suboxic zone Δ*L*. (C) The electric potential signal ΔEP. Cable bacteria activity was observed in 3 out of 4 destination cores at different time points (DC1: Day 54, DC4: Day 75 and DC3: Day 85). The markers (dots) are the parameter values calculated from individual profiles. Multiple spots were profiled, resulting in four data points per timepoint for the natural sediment (black markers) and two data points for the destination cores (coloured markers). The line connects the average parameter value across replicate profiles at each single time point.

**TABLE 1** Cable bacteria presence and diversity in destination cores and estimated time of colonisation.

| Destination core | Sampling day | Volumetric filament density (m/cm$^3$) | Areal density (m/cm$^2$) | Total filament length in core (m) | # generations | Estimated day of colonisation | Observed ASVs | Shannon index |
|---|---|---|---|---|---|---|---|---|
| DC1 | 54 | 211 | 49 | 618 | 14 | 42 | 253 | 3.7 |
| DC2 | 85 | 29 | 7 | 84 | 12 | 74 | 185 | 3.2 |
| DC3 | 85 | 375 | 210 | 2622 | 16 | 71 | 156 | 3.5 |
| DC4 | 85 | 252 | 186 | 2327 | 15 | 71 | 180 | 3.5 |

*Note*: The sampling day marks the first detection of the geochemical fingerprint. Volumetric filament density was analysed by FISH and used to calculate the areal density and total filament length in a core. Using the observed median filament snippet size of 15 cells, the number of generations needed to reach the observed filament density was estimated. The number of observed ASVs and Shannon index were based on amplicon sequence data for 2–6 mm sediment depth.

minimum ($\Delta$pH = 0.3), a developing suboxic zone ($\Delta L$ = 1.3 mm) and a non-zero EP signal ($\Delta$EP = 0.2 mV). At this time point, the other destination cores (DC2 to DC4) did not show any cable bacteria activity. At Day 75, a second destination core (DC4) showed cable bacteria activity ($\Delta$pH = 0.5; $\Delta L$ = 2.4 mm; $\Delta$EP = 0.2 mV), and 10 days later, DC3 also had developed the cable bacteria geochemical fingerprint ($\Delta$pH = 1.0; $\Delta L$ = 5.7 mm, $\Delta$EP = 0.2 mV). At this point (85 days), the experiment was terminated, and the remaining fourth destination core (DC2) did not show a clear geochemical fingerprint, but a small $\Delta$EP increase was noticeable (Figure 2).

At the sampling day (i.e., when the geochemical fingerprint of cable bacteria activity was first detected; Table 1), the three destination cores (DC1, DC3 and DC4) showed a high volumetric filament density, ranging between 211 and 375 m cm$^{-3}$ (Table 1). While DC2 did not show a clear cable bacteria fingerprint at the end of the experiment, it still had a notable volumetric filament density (29 m cm$^{-3}$ sediment), which suggested that successful dispersal had occurred. Likely, the population was not yet dense/active enough to generate the distinct geochemical fingerprint. Previous studies have shown that the fingerprint only appears when the population is firmly established (Geelhoed et al., 2020). In the two negative controls, the fingerprint did not appear over the 85-day experimental period and no cable bacteria were detected by FISH after 54 and 85 days of incubation.

## Detection of cable bacteria in the overlying water

To investigate dispersion through the water column, FISH was applied to overlying water samples at five time points throughout the experiment. At the start of the experiment, no cable bacteria could be detected, but from Day 14 onwards, filament fragments ('snippets') appeared in the overlying water (Figure 3A). The areal snippet density (expressed per cm$^2$ of natural 'source' sediment) increased by a factor of 5 throughout the experiment (from 0.09 m cm$^{-2}$ on Day 14 to 0.41 m cm$^{-2}$ on Day 85; Table 2). This demonstrates a progressive accumulation of snippets in the water column, which was not refreshed during the experiment. The accumulation of snippets was linear in time (Figure 3B), and consequently, the release rate of cable bacteria snippets remained roughly constant throughout the experiment (51–81 cells h$^{-1}$ cm$^{-2}$; Figure 3B).

Notably, fine sediment particles were found floating in the overlying water, and accumulated on the bottom of the microcosm. Most likely, a small amount of

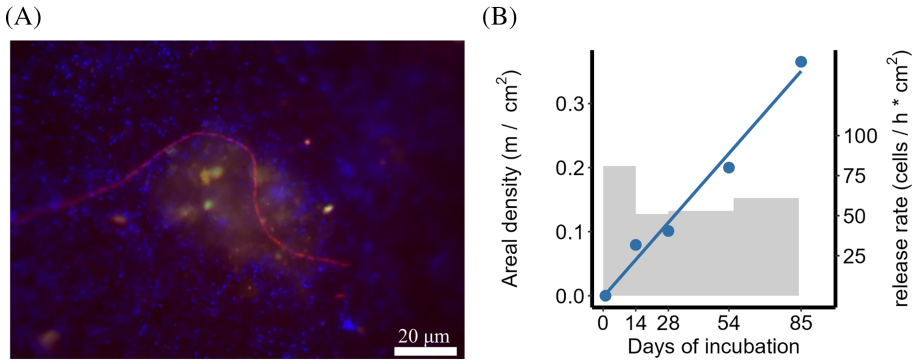


**FIGURE 3** Cable bacteria detection in the overlying water. (A) Cable bacteria in the overlying water assessed by FISH with the DSB706 probe (red) and counterstained with DAPI (blue). Cable bacteria occurred in short fragments ('snippets') of 8–21 cells, appeared to be attached to sediment particles and were surrounded by many other microbes. The observed yellow colour arose from the autofluorescence of a sediment particle. The scale bar depicts 20 µm. (B) Volumetric filament density of cable bacteria in the overlying water (blue markers, left *y*-axis) shows an increase over time (line: $r^2 = 0.98$). The associated cell release rate from the natural sediment remains relatively constant over time (grey bars).

**TABLE 2** Cable bacteria filament fragments were detected in the overlying water of the mesocosm and in situ overlying water sampled at low tide.

| Sample | Day | Volumetric filament density (mm $cm^{-3}$ OW) | Areal density (m $cm^{-2}$) | Fragment length Median (observed range) (µm) | Estimated number of cells per fragment median (observed range) (#) | Fragments attached to sediment (%) | Net cell release rate (cells $h^{-1}$ $cm^{-2}$) |
|---|---|---|---|---|---|---|---|
| OW | 1 | 0 | 0 | 0 (0) | 0 | 0 | 0 |
| OW | 14 | 0.79 | 0.09 | 62 (26–200) | 21 (8–61) | 0 | 81 |
| OW | 28 | 1.01 | 0.11 | 36 (7–252) | 12 (2–76) | 0 | 51 |
| OW | 54 | 2 | 0.23 | 25 (9–173) | 8 (3–52) | 29 | 53 |
| OW | 85 | 3.65 | 0.41 | 59 (16–203) | 20 (5–62) | 33 | 61 |
| in situ OW | | 0.54 | 0.001 | 13 (7–70) | 4 (2–21) | 58 | 51 |

Abbreviation: OW, overlying water.

sediment resuspension was induced by the currents in the overlying water (caused by the bubble-type aeration). Analysing the FISH images in closer detail, we noticed that part of the snippets were 'free-floating', while others were attached to sediment particles, often together with organic debris and single-celled bacteria (Figure 3A). Initially, all observed snippets were free-floating, but with longer incubation time (at Days 54 and 85), ~30% of filaments in the overlying water were attached to sediment particles (Table 2). The median snippet length found in the overlying water of the microcosm varied between 25 and 62 µm, with no clear pattern with time. The observed size of snippets was 3–77 cells, with an overall median of 15 ± 6 cells.

## The time window of colonisation

The filament densities recorded in the destination cores enable a crude estimate of the colonisation time. Assuming a constant doubling time of $t_d = 20$ h (Schauer et al., 2014) and assuming that all cells divide at the same time, the development time can be estimated as $\tau = N \times t_d$, where $N$ represents the number of generations since the moment of colonisation. Assuming exponential growth, $N = \ln(C_t/C_0)/\ln(2)$, where $C_t$ is the number of cells present in the destination core and $C_0$ is the number of cells that originally inoculated the sediment. The value of $C_t = \rho_{area,sed}/L_{cell}$ (cells $cm^{-2}$) was calculated from the areal filament density recorded by FISH. The value of $C_0 = N_{snippet}/A_{sed}$, was calculated from the surface area of the destination core $A_{sed}$ and the mean snippet length observed in the water, $N_{snippet} = 15$ cells, assuming that a colonisation event occurred only once. From this, we estimate that it would have taken ~10–13 generations to reach the observed cable bacteria filament density (Table 1), suggesting that inoculation happened at Day 42 for DC1, Day 71 for DC4 and Day 71 for DC3 (Table 1). For destination core (DC2), inoculation happened around Day 74, which then resulted in a small increase in ΔEP on Day 85.

## Detecting cable bacteria in the destination cores using 16S rRNA gene amplicon sequencing

The microbial community of sediment and overlying water samples was analysed by sequencing the V3–V4 region of the 16S rRNA gene. The total number of counts per sample ranged from 26,500 to 144,400, resulting in a detection limit of 0.01–0.04%. NMDS analysis showed that samples were grouped together in distinct clusters (Figure 4A), with the overlying water being distant from the sediment samples. The natural sediment samples taken at different time points clustered tightly together, indicating no effect of incubation time, and grouped separately from the destination cores and negative controls. The stress value for the NMDS analysis was 0.03, indicating a good fit of the data to the two-dimensional representation.

At the beginning of the experiment, the natural sediment showed the highest observed ASVs (1035), which declined throughout the experiment (574 by Day 85; Figure 4B). The Shannon index, a measure considering both ASV richness and evenness, exhibited a similar pattern (Figure 4C). At the time of first detection of the cable bacteria activity, the destination cores showed a markedly lower number of observed ASVs (Figure 4B) and Shannon index (Figure 4C), indicative of a less complex community. The negative control samples showed the lowest observed number of ASVs and Shannon diversity index. At the start of the experiment, the microbial community in the overlying water showed the lowest ASV richness (75 ASVs), but became more diverse over time, increasing to 305 ASVs on Day 54, and attaining 270 ASVs on Day 85.

In total, three *Ca.* Electrothrix ASVs were detected across all samples (ASV-CB1, ASV-CB2 and ASV-CB3). ASV-CB1 was 99.3% identical to the 16S rRNA gene V3–V4 sequence of *Ca.* E. laxa (Sereika et al., 2023), ASV-CB2 was identical to *Ca.* E. rattekaaiensis (Plum-Jensen et al., 2024) and ASV-CB3 was 99.8% identical to cable bacteria enrichment culture clone WH1-7 (Larsen et al., 2015). In the natural sediment at the start of the experiment, cable bacteria were not detectable using 16S rRNA sequencing, even though cable bacteria were detected using FISH. On Day 54, ASV-CB2 showed a relative abundance of 0.3%, while ASV-CB1 and ASV-CB3 were not detected. At Day 85, the relative abundance of ASV-CB2 decreased to 0.1%, whereas the relative abundance of ASV-CB3 increased to 0.4%. ASV-CB1 was not found in the natural sediment at any of the three time points. The relative abundance of cable bacteria appeared relatively low, possibly because cable bacteria growth had peaked between Days 14 and

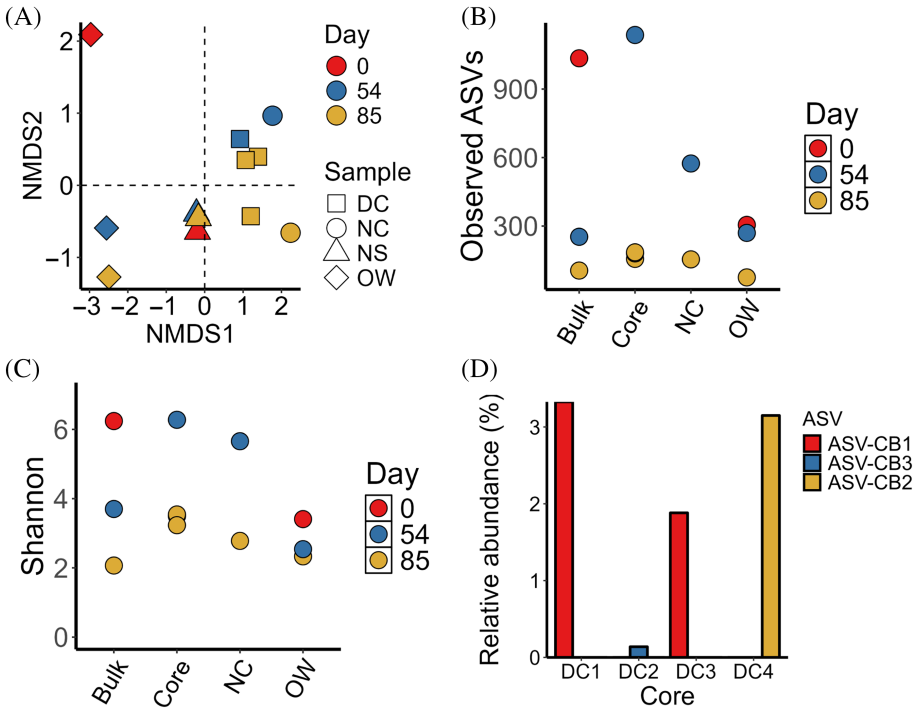


**FIGURE 4** Diversity analysis of the sediment (2–6 mm depth) and overlying water microbial communities based on V3–V4 16S rRNA gene amplicon analysis. (A) Non-metric multidimensional scaling (NMDS) plot of the microbial communities across all samples with sample type shown with different shapes and days of incubation displayed with different colours. Diversity indexes (B) observed ASVs and (C) Shannon calculated on rarefied datasets for the different samples, with data points for different days of incubation in different colours. (D) V3–V4 16S rRNA gene amplicon analysis revealed the presence of a single cable bacterium ASV per destination core. Sampling times: DC1: Day 54; DC2, DC3, DC4: Day 85. NS, natural sediment; DC, destination cores; OW, overlying water; NC, negative controls.

28 (Figure 2) before sediment samples were taken for ASV and FISH analysis, and/or because cable bacteria growth may be patchy thus resulting in spatial heterogeneity (Yin et al., 2021).

The three destination cores that showed colonisation had a relative abundance of cable bacteria ASVs of 2%–3%, which is markedly higher compared to the natural source sediment. Note, however, that samples were taken from the top 4 mm in the natural sediment, and from the suboxic zone (2–6 mm) in the destination cores. In the oxic zone, cable bacteria typically show a lower relative ASV abundance compared to deeper layers due to the overall elevated abundance of many aerobic bacteria (Geelhoed et al., 2020). The lower complexity of the community may also help explain the higher relative abundance of cable bacteria in the destination cores. Autoclaving the sediment decreased the microbial complexity and the number of ASVs and Shannon index were similar to those described previously for autoclaved sediment, in which the community was largely reduced to spore-forming members of the phylum *Bacillota* (>96%) (Hiralal et al., 2024). Even though multiple cable bacteria ASVs were present in the source sediment, each colonised destination core showed only a single cable bacterium ASV (Figure 4). While DC4 showed the presence of ASV-CB2, DC1 and DC3 contained ASV-CB1. The fourth destination core, DC2, exhibited a lower relative abundance of 0.14% of ASV-CB3. The low relative abundance is in agreement with the FISH analysis (Figure 3 and Table 1). Cable bacteria ASV-CB1 and ASV-CB3 were also detected in the overlying water on Day 85. No cable bacteria ASVs were detected in the negative controls.

## Field sampling

The laboratory experiment revealed a release of cable bacteria snippets to the overlying water. To verify whether a similar process occurs under natural conditions, we performed field sampling in a salt marsh creek. The creek was the same site as where the natural sediment for the laboratory experiment was collected 8 months earlier. At low tide, the creek bed contained a local pool with a shallow layer of stagnant seawater (height $\sim$ 2 cm) overlying the sediment. The creek bed pool had a total surface area of $\sim$9 $m^2$ (Figure 1C). Microsensor profiling at six locations in the creek bed revealed the fingerprint of metabolic activity by cable bacteria (Figure 5A) with $\Delta$EP values ranging from 0.4–0.8 mV. The suboxic zone stretched to 15 mm depth, and the subsurface pH minimum was 5.8, all indicative of strong in situ e-SOx activity. FISH revealed a volumetric filament density of 209 m $cm^{-3}$ in the sediment, which amounted to an areal filament density of 261 m $cm^{-2}$, which is larger than the areal densities found in the laboratory incubation (50–209 m $cm^{-3}$) and the 140 m $cm^{-2}$ previously found under in situ conditions in Rattekaai salt marsh (Malkin et al., 2014). In the overlying water of the creek, the volumetric filament density was $\rho_{creek} = 0.54$ mm $cm^{-3}$, of which 58% of the filaments were attached to sediment particles. Knowing that the water in the creek bed is refreshed every 12.4 h on average by the tide, and that we sampled during low tide ($\Delta t = 6$ h of accumulation) and accounting for the water height $H_{creek} = 2$ cm and the cell length $L_{cell} = 3.3$ µm, we calculated a cable bacterium release rate of

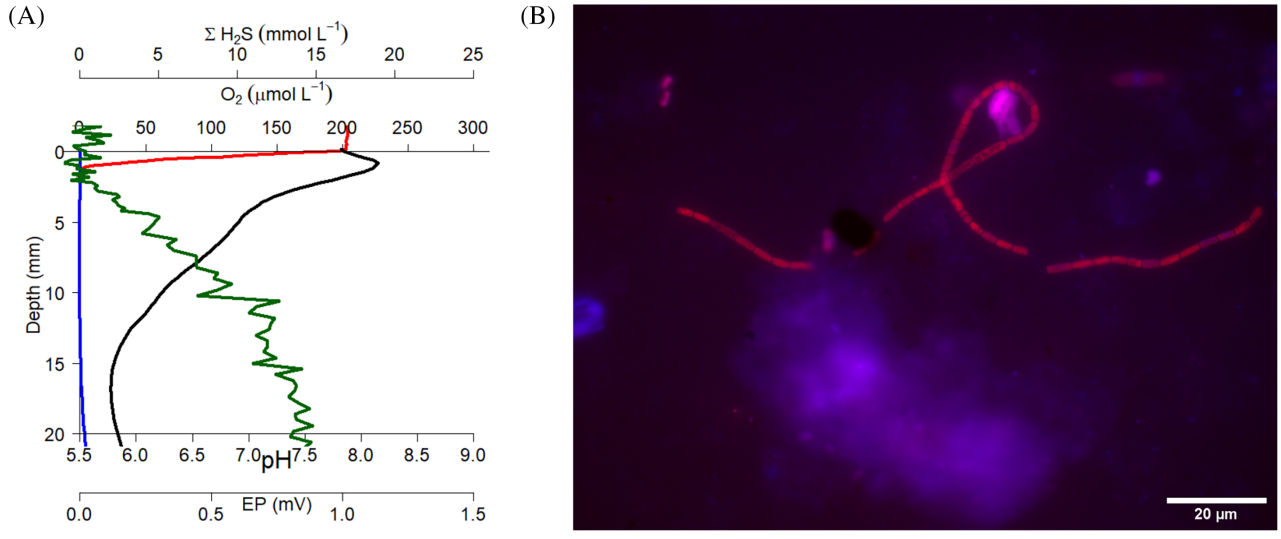


FIGURE 5 Cable bacteria were present in both sediment and creek bed water of the Rattekaai salt marsh. (A) Microsensor profiles of oxygen (red), pH (black), sulphide (blue) and electric potential (green) of an in situ core. (B) One cable bacterium snippet present in situ overlying water stained with FISH using the DSB706 probe (red) and counterstained with DAPI. A piece of the filament is not visible behind a sediment particle and two empty cells cause a kink in the filament. The scale bar depicts 20 µm.

$$R_{cell} = \rho_{creek} \times H_{creek} / (\Delta t \times L_{cell})$$

to be 51 cells $h^{-1}$ $cm^{-2}$ sediment, which is comparable to the release rate observed in the laboratory experiment (Figure 3B).

## DISCUSSION

Our results show that cable bacteria can disperse through an oxygenated water column and colonise new sediment areas. In our mesocosm setup, the natural source sediment developed strong cable bacteria activity within 14 days. Destination cores were filled with autoclaved sediment and were positioned ~6–11 cm away from the source sediment, only reachable by transfer through the water (Figure 1). Cable bacteria activity developed in the destination cores after 54–85 days. Short filament fragments of cable bacteria (snippets of 3–77 cells) were detected in the overlying water from early on (Day 14; Table 1). However, successful inoculation occurred only much later, approximately between Days 42 and 71. The number of snippets in the water column increased over time, and an increasing fraction of these snippets was found attached to sediment particles. Both factors may have increased the colonisation's success. While increased snippet concentration in the overlying water may increase the likelihood or success of an inoculation event, attachment to sediment particles may especially contribute to the latter by retaining the viability of cable bacteria cells upon passage through the oxygenated water column (Figure 6B). The total length of filament released from the source sediment over the 85-day experiment amounted to ~66 m (Table 2), which is equivalent to ~1.3 million snippets.

Over the same period, our results suggest that only 4 successful colonisation events occurred in the destination cores. The high amounts of snippets released to the water column (~1.3 million snippets released over 85 days) versus the small number of colonisation events indicates that colonisation is a rare event. Only a single ASV, out of multiple cable bacteria ASVs present in the natural source sediment, was found to develop in each of the destination cores, with different ASVs developing in different cores (Figure 4D). This 'founder effect' suggests that a single colonisation event lies at the base of each observed successful population development. Most likely, colonisation results from the successful settlement of one (or at most a few) individuals of the same ASV, subsequently followed by filament elongation and multiplication of filaments (Geelhoed et al., 2020; Schauer et al., 2014). If multiple filaments would synchronously colonise a sediment core, then it becomes statistically improbable they would belong to a single ASV. Moreover, the fact that different ASVs colonised different destination cores suggests that colonisation events are intrinsically stochastic in nature. If the geochemical environment of the autoclaved sediment of the destination cores would favour colonisation of one particular ASV, then one would expect to see the same ASV in all destination cores.

Our results suggest that the dispersal of cable bacteria occurs via snippets through the water column. However, it is currently unknown if cable bacteria can also exist and disperse as single cells. Note that by using FISH with probe DSB706 we would not be able to distinguish between cable bacteria in a single cell stage and other members of the *Desulfobulbaceae* family. If we assume that colonisation occurs by a single snippet, the chance that a given snippet released from the source sediment also accomplishes effective

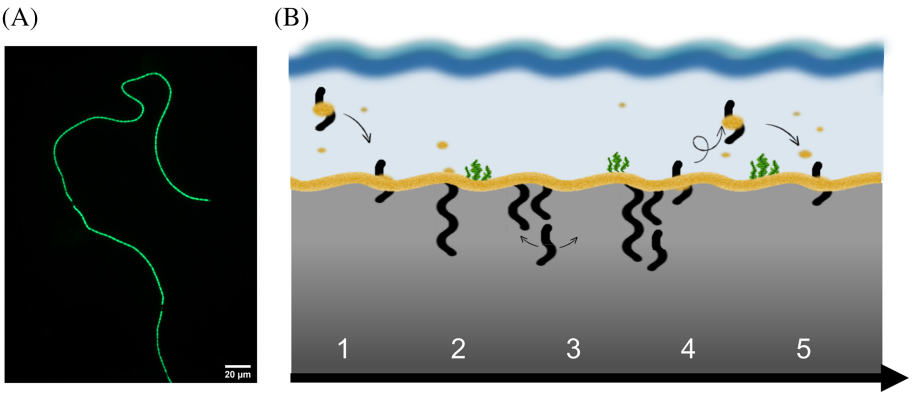


**FIGURE 6** (A) Image of a cable bacterium hybridised with probe EUB338-Cy3 in which some cells appear to be empty (white arrows). The scale bar depicts 20 µm. (B) Proposed model of effective dispersal of cable bacteria. (1) A cable bacterium 'snippet' attached to a sediment particle colonises the sediment and (2) grows in the sediment. (3) Cable bacterium breakage, possibly due to sacrificial cell death, produces fragments that utilise gliding motility to reach the oxic layer and grow and develop into a population. (4) A short fragment or 'snippet' attached to a sediment particle is released into the water column. (5) The 'snippet' settles at a favourable location and the effective dispersal event restarts the cycle.

dispersal amounts to ~0.0003%, thus showing that there is a very small chance for a snippet to successfully colonise a new sediment environment. The fact that only a single filament can lead to successful population development, is experimentally supported by so-called clonal culturing (Hiralal et al., 2024; Li et al., 2022; Thorup et al., 2021), which is based on the transfer of a single filament.

The successful establishment also depends on suitable geochemical conditions and priority effects, that is, a prior occupation that impacts the establishment of a new coloniser (Hanson et al., 2012). Whether or not the existing microbial community at a new location impacts the successful establishment of cable bacteria is currently unknown. It has been hypothesised that other microorganisms might interact with cable bacteria through the transfer of electrons for respiration, but the exact mechanism of this interspecies electron transfer and whether this process could be beneficial to cable bacteria requires further study (Bjerg et al., 2023; Vasquez-Cardenas et al., 2015). However, if interactions between cable bacteria and other microorganisms would be mutualistic, then these associated microorganisms must either be cotransferred along with the cable bacteria, or they must be already present in the new environment. This could hence decrease the rate of successful colonisation. Moreover, it should be noted that in this laboratory study, autoclaved sediment was used in the destination cores, thus implying that the ecological niche for cable bacteria was entirely vacant. However, under in situ conditions, this same niche could already be occupied by 'indigenous' cable bacteria, thus making it potentially harder for other cable bacteria strains to colonise this sediment.

Together, our results provide the following tentative model of how cable bacteria colonise new sediments (Figure 6B). (1) A single viable snippet lands on the sediment surface and subsequently grows into a longer filament that penetrates deeper into the sediment. Cable bacteria divide along the length of the filament that is located in the suboxic zone (Geerlings et al., 2020; Schauer et al., 2014). Therefore, starting from 15 cells (mean snippet length), it takes about 9 generations to reach a filament that is ~1 cm long (~3000 cells). (2) A growing 'founder filament' occasionally breaks and produces daughter filaments, which each must migrate upwards to the oxic–anoxic interface, to get back into contact with $O_2$, which is required as an electron acceptor. As demonstrated, cable bacteria indeed possess a gliding motility (velocity 0.5–1 $\mu m\ s^{-1}$), likely driven by chemotaxis, which enables filament fragments to reposition (Bjerg et al., 2016). The process of filament fragmentation is less clear but seems an essential requirement for one initial founder filament to create a whole population of filaments. Effectively, cable bacteria could possess a similar filament multiplication mechanism as filamentous sulphur-oxidizing *Beggiatoa*, which display sacrificial cell death resulting in cell lysis followed by filament breakage (Kamp et al., 2008). This breakage occurs within a stretched filament, within a loop, or at the position where the loop was formerly located in the trichome. Sacrificial cell death can occur in several places in a filament, resulting in more daughter filaments (Strohl & Larkin, 1978). In cable bacteria, loop formation has been linked to gliding motility (Bjerg et al., 2016) but could have an additional role in generating suitable breakpoints. Notably, in FISH images, not all cable bacteria cells are stained, which indicates that these are not viable (Figure 5B, 6A), and hence, could potentially act as sites of breakage. Additionally, the occurrence of lysed cells in cable bacteria filaments has been observed using nanoSIMS (Geerlings et al., 2020); however, it was unclear whether this was due to damage resulting from handling the filaments or whether this had occurred naturally. Note that if the mechanism of sacrificial cell death occurs in cable bacteria, the periplasmic fibres also need to break to obtain daughter filaments and, hence, an increase in the density of filaments over time. Other processes that could cause or contribute to filament fragmentation and sediment particle release are shearing stress due to water movement and perhaps the gliding movement of cable bacteria themselves in the sediment. In natural conditions, the impact of shearing stress will be much larger compared to the mesocosm experiment due to currents and wave action and as a result of bioturbating fauna that causes mixing of the upper centimetres of the sediment (Christiansen et al., 2000; Kristensen et al., 2012; Nowacki & Ogston, 2013). For environments like salt marshes that fall (almost) dry during low tide, the spreading of sediment attached to birds' feet could also contribute to the dispersal of microorganisms (Green et al., 2023).

(3) Filament fragmentation is also required to release snippets into the water column. This implies that these snippets migrate across the oxic zone of the sediment and are released into the overlying water. The effective dispersal of cable bacteria through a fully oxygenated water column is remarkable, as cable bacteria can be regarded as microaerophilic bacteria (Bjerg et al., 2018; Scilipoti et al., 2021) and exposure to oxygen rapidly irreversibly diminishes the conductance of cable bacterium filaments (Meysman et al., 2019). At the sediment–water interface, cable bacteria perform oxygen reduction at a very high rate (Geerlings et al., 2019; Scilipoti et al., 2021), however, this is only a small part of the filament. Furthermore, cable bacteria are closely related to anaerobic sulphate-reducing bacteria (Kjeldsen et al., 2019) and hence oxygen likely inhibits many enzymatic processes. The encapsulation of cable bacteria filament fragments in sediment particles may protect the cells from oxygen in the water column and increase their

viability. Some species of cable bacteria encode canonical cytochrome c oxidase, which may contribute to the scavenging of oxygen (Hiralal et al., 2024; Kjeldsen et al., 2019; Sereika et al., 2023). In addition, utilisation of energy stored in the form of polyphosphate granules (Geerlings et al., 2022; Kjeldsen et al., 2019) may also improve the chances of survival. Thus, the successful establishment of cable bacteria in a new location can be explained by the transport of cable bacteria snippets via the water phase, likely protected by the environment of a sediment particle.

This would also ease the geographical spread of cable bacteria and explain why we can find the same species in opposite parts of the world. Although transport of snippets via the water phase driven by large-scale processes like currents could in principle cover large distances, the duration for which a snippet can remain viable even when protected by a sediment particle will be limited. Hence effective dispersal to a nearby location is more likely than further away, resulting in dispersal limitation (Hanson et al., 2012). In oceans and freshwater systems, microorganisms exhibit diverse interactions with particle surfaces; some may transiently colonise particles, while others establish enduring and stable colonies (Ebrahimi et al., 2022). Organic particles that harbour microbial communities may promote a vertical connection between surface and deep-sea microbial communities (Mestre et al., 2018). The cable bacteria dispersal mechanism could be exploited or optimised to promote cable bacteria growth in environments that may benefit from cable bacteria presence, for example, in the case of rice paddies, where cable bacteria activity has been shown to suppress methane emissions (Scholz et al., 2020).

To summarise, we suggest cable bacteria may benefit from attachment to sediment particles as a vehicle for dispersal and as protection against the oxic overlying water (Figure 6B). Initially, the cable bacteria colonise a given location. The cable bacteria grow deeper into the sediment and filament snippets are produced for filament multiplication and are also released into the overlying water. Snippets attached to sediment particles are transported in the water column and colonise new areas.

## AUTHOR CONTRIBUTIONS

**Jesper R. van Dijk:** Conceptualisation; investigation; writing – original draft; writing – review and editing; visualisation; formal analysis. **Jeanine S. Geelhoed:** Supervision; conceptualisation; writing – review and editing. **Philip Ley:** Investigation; writing – review and editing. **Silvia Hidalgo-Martinez:** Investigation. **Miguel Portillo-Estrada:** Investigation. **Erik Verbruggen:** Writing – review and editing; supervision. **Filip J. R. Meysman:** Conceptualisation; supervision; writing – review and editing; funding acquisition.

## ACKNOWLEDGEMENTS

The research is financially supported by the Research Foundation Flanders (FWO grant S004523N) and the University of Antwerp via the TopBOF program. JRvD received a PhD scholarship via the Dehousse program from the University of Antwerp. FJRM received additional support from the European Innovation Council (Pathfinder project 101046719 PRINGLE).

## CONFLICT OF INTEREST STATEMENT

The authors declare no conflicts of interest.

## DATA AVAILABILITY STATEMENT

V3-V4 amplicon sequence data have been submitted to the European Nucleotide Archive under BioProject number PRJEB73801: https://www.ebi.ac.uk/ena/browser/view/PRJEB73801. Geochemical data and supplementary files are available from the Zenodo repository: https://zenodo.org/doi/10.5281/zenodo.13140734.

## ORCID

*Jesper R. van Dijk* https://orcid.org/0000-0002-2449-600X
*Jeanine S. Geelhoed* https://orcid.org/0000-0001-6334-2604
*Philip Ley* https://orcid.org/0000-0002-7940-7641
*Silvia Hidalgo-Martinez* https://orcid.org/0009-0005-1878-0361
*Miguel Portillo-Estrada* https://orcid.org/0000-0002-0348-7446
*Erik Verbruggen* https://orcid.org/0000-0001-7015-1515
*Filip J. R. Meysman* https://orcid.org/0000-0001-5334-7655

## REFERENCES

Barbour, K.M., Barrón-Sandoval, A., Walters, K.E. & Martiny, J.B.H. (2023) Towards quantifying microbial dispersal in the environment. *Environmental Microbiology*, 25, 137–142.

Barnett, J.M., Arts, I.C.W. & Penders, J. (2021) microViz: an R package for microbiome data visualization and statistics. *Journal of Open Source Software*, 6(63), 3201.

Becking, B. (1934) *Geobiologie of inleiding tot de milieukunde*. The Hague: W. P. Van Stockum & Zoon.

Bjerg, J.J., Lustermans, J.J.M., Marshall, I.P.G., Mueller, A.J., Brokjaer, S., Thorup, C.A. et al. (2023) Cable bacteria with electric connection to oxygen attract flocks of diverse bacteria. *Nature Communications*, 14, 1614.

Bjerg, J.T., Boschker, H.T.S., Larsen, S., Berry, D., Schmid, M., Millo, D. et al. (2018) Long-distance electron transport in individual, living cable bacteria. *Proceedings of the National Academy of Sciences of the United States of America*, 115, 5786–5791.

Bjerg, J.T., Damgaard, L.R., Holm, S.A., Schramm, A. & Nielsen, L.P. (2016) Motility of electric cable bacteria. *Applied and Environmental Microbiology*, 82, 3816–3821.

Burdorf, L.D.W., Malkin, S.Y., Bjerg, J.T., van Rijswijk, P., Criens, F., Tramper, A. et al. (2018) The effect of oxygen availability on long-distance electron transport in marine sediments. *Limnology and Oceanography*, 63, 1799–1816.

Burdorf, L.D.W., Tramper, A., Seitaj, D., Meire, L., Hidalgo-Martinez, S., Zetsche, E.M. et al. (2017) Long-distance electron

transport occurs globally in marine sediments. *Biogeosciences*, 14, 683–701.

Callahan, B.J., McMurdie, P.J., Rosen, M.J., Han, A.W., Johnson, A.J.A. & Holmes, S.P. (2016) DADA2: high-resolution sample inference from Illumina amplicon data. *Nature Methods*, 13, 581.

Cho, J.C. & Tiedje, J.M. (2000) Biogeography and degree of endemicity of fluorescent strains in soil. *Applied and Environmental Microbiology*, 66, 5448–5456.

Christiansen, T., Wiberg, P.L. & Milligan, T.G. (2000) Flow and sediment transport on a tidal salt marsh surface. *Estuarine, Coastal and Shelf Science*, 50, 315–331.

Custer, G.F., Bresciani, L. & Dini-Andreote, F. (2022) Ecological and evolutionary implications of microbial dispersal. *Frontiers in Microbiology*, 13, 855859.

Dam, A.S., Marshall, I.P.G., Risgaard-Petersen, N., Burdorf, L.D.W. & Marzocchi, U. (2021) Effect of salinity on cable bacteria species composition and diversity. *Environmental Microbiology*, 23, 2605–2616.

Damgaard, L.R., Risgaard-Petersen, N. & Nielsen, L.P. (2014) Electric potential microelectrode for studies of electrobiogeophysics. *Journal of Geophysical Research: Biogeosciences*, 119, 1906–1917.

de Wit, R. & Bouvier, T. (2006) 'Everything is everywhere, but, the environment selects'; what did Baas Becking and Beijerinck really say? *Environmental Microbiology*, 8, 755–758.

Duvallet, C., Gibbons, S.M., Gurry, T., Irizarry, R.A. & Alm, E.J. (2017) Meta-analysis of gut microbiome studies identifies disease-specific and shared responses. *Nature Communications*, 8, 1784.

Ebrahimi, A., Goyal, A. & Cordero, O.X. (2022) Particle foraging strategies promote microbial diversity in marine environments. *eLife*, 11, e73948.

Fenchel, T. & Finlay, B.J. (2004) The ubiquity of small species: patterns of local and global diversity. *BioScience*, 54, 777–784.

Geelhoed, J.S., Thorup, C.A., Bjerg, J.J., Schreiber, L., Nielsen, L.P., Schramm, A. et al. (2023) Indications for a genetic basis for big bacteria and description of the giant cable bacterium *Candidatus Electrothrix gigas* sp. nov.. *Microbiology Spectrum*, 11:e0053823.

Geelhoed, J.S., van de Velde, S.J. & Meysman, F.J.R. (2020) Quantification of cable bacteria in marine sediments via qPCR. *Frontiers in Microbiology*, 11, 1506.

Geerlings, N.M.J., Karman, C., Trashin, S., As, K.S., Kienhuis, M.V.M., Hidalgo-Martinez, S. et al. (2020) Division of labor and growth during electrical cooperation in multicellular cable bacteria. *Proceedings of the National Academy of Sciences of the United States of America*, 117, 5478–5485.

Geerlings, N.M.J., Kienhuis, M.V.M., Hidalgo-Martinez, S., Hageman, R., Vasquez-Cardenas, D., Middelburg, J.J. et al. (2022) Polyphosphate dynamics in cable bacteria. *Frontiers in Microbiology*, 13, 883807.

Geerlings, N.M.J., Zetsche, E.M., Hidalgo-Martinez, S., Middelburg, J.J. & Meysman, F.J.R. (2019) Mineral formation induced by cable bacteria performing long-distance electron transport in marine sediments. *Biogeosciences*, 16, 811–829.

Green, A.J., Lovas-Kiss, A., Reynolds, C., Sebastian-González, E., Silva, G.G., van Leeuwen, C.H.A. et al. (2023) Dispersal of aquatic and terrestrial organisms by waterbirds: a review of current knowledge and future priorities. *Freshwater Biology*, 68, 173–190.

Hanson, C.A., Fuhrman, J.A., Horner-Devine, M.C. & Martiny, J.B.H. (2012) Beyond biogeographic patterns: processes shaping the microbial landscape. *Nature Reviews Microbiology*, 10, 497–506.

Herlemann, D.P.R., Labrenz, M., Jürgens, K., Bertilsson, S., Waniek J.J. & Andersson A. F. (2011) Transitions in bacterial communities along the 2000 km salinity gradient of the Baltic Sea. ISME Journal. 5, 1571-1579.

Hiralal, A., Geelhoed, J.S., Hidalgo-Martinez, S., Smets, B., van Dijk, J.R. & Meysman, F.J.R. (2024) Closing the genome of unculturable cable bacteria using a combined metagenomic assembly of long and short sequencing reads. *Microbial Genomics*, 10, 001197.

Kamp, A., Roy, H. & Schulz-Vogt, H.N. (2008) Video-supported analysis of *Beggiatoa* filament growth, breakage, and movement. *Microbial Ecology*, 56, 484–491.

Kjeldsen, K.U., Schreiber, L., Thorup, C.A., Boesen, T., Bjerg, J.T., Yang, T.T. et al. (2019) On the evolution and physiology of cable bacteria. *Proceedings of the National Academy of Sciences of the United States of America*, 116, 19116–19125.

Kristensen, E., Penha-Lopes, G., Delefosse, M., Valdemarsen, T., Quintana, C.O. & Banta, G.T. (2012) What is bioturbation? The need for a precise definition for fauna in aquatic sciences. *Marine Ecology Progress Series*, 446, 285–302.

Lahti, L. & Shetty, S. (2012–2019) microbiome R package.

Larsen, S., Nielsen, L.P. & Schramm, A. (2015) Cable bacteria associated with long-distance electron transport in New England salt marsh sediment. *Environmental Microbiology Reports*, 7, 175–179.

Li, C., Reimers, C.E. & Chace, P.J. (2022) Protocol for using autoclaved intertidal sediment as a medium to enrich marine cable bacteria. *STAR Protocols*, 3, 101604.

Loy, A., Lehner, A., Lee, N., Adamczyk, J., Meier, H., Ernst, J., et al. (2002). Oligonucleotide microarray for 16S rRNA gene-based detection of all recognized lineages of sulfate-reducing prokaryotes in the environment. Applied and Environmental Microbiology, 68, 5064–5081.

Lücker, S., Steger, D., Kjeldsen, K.U., MacGregor, B.J., Wagner, M. & Loy, A. (2007). Improved 16S rRNA-targeted probe set for analysis of sulfate-reducing bacteria by fluorescence in situ hybridization. Journal of Microbiological Methods, 69, 523-528.

Malkin, S.Y., Rao, A.M.F., Seitaj, D., Vasquez-Cardenas, D., Zetsche, E.M., Hidalgo-Martinez, S. et al. (2014) Natural occurrence of microbial sulphur oxidation by long-range electron transport in the seafloor. *The ISME Journal*, 8, 1843–1854.

Marzocchi, U., Bonaglia, S., van de Velde, S., Hall, P.O.J., Schramm, A., Risgaard-Petersen, N. et al. (2018) Transient bottom water oxygenation creates a niche for cable bacteria in long-term anoxic sediments of the Eastern Gotland Basin. *Environmental Microbiology*, 20, 3031–3041.

Marzocchi, U., Trojan, D., Larsen, S., Meyer, R.L., Revsbech, N.P., Schramm, A. et al. (2014) Electric coupling between distant nitrate reduction and sulfide oxidation in marine sediment. *The ISME Journal*, 8, 1682–1690.

McMurdie, P.J. & Holmes, S. (2013) Phyloseq: an R package for reproducible interactive analysis and graphics of microbiome census data. *PLoS One*, 8, e61217.

Mestre, M., Ruiz-González, C., Logares, R., Duarte, C.M., Gasol, J.M. & Sala, M.M. (2018) Sinking particles promote vertical connectivity in the ocean microbiome. *Proceedings of the National Academy of Sciences of the United States of America*, 115, E6799–E6807.

Meysman, F.J.R., Cornelissen, R., Trashin, S., Bonne, R., Martinez, S.H., van der Veen, J. et al. (2019) A highly conductive fibre network enables centimetre-scale electron transport in multicellular cable bacteria. *Nature Communications*, 10, 4120.

Meysman, F.J.R., Risgaard-Petersen, N., Malkin, S.Y. & Nielsen, L.P. (2015) The geochemical fingerprint of microbial long-distance electron transport in the seafloor. *Geochimica et Cosmochimica Acta*, 152, 122–142.

Nielsen, L.P., Risgaard-Petersen, N., Fossing, H., Christensen, P.B. & Sayama, M. (2010) Electric currents couple spatially separated biogeochemical processes in marine sediment. *Nature*, 463, 1071–1074.

Nikodemova, M., Holzhausen, E.A., Deblois, C.L., Barnet, J.H., Peppard, P.E., Suen, G. et al. (2023) The effect of low-

abundance OTU filtering methods on the reliability and variability of microbial composition assessed by 16S rRNA amplicon sequencing. *Frontiers in Cellular and Infection Microbiology*, 13, 1165295.

Nowacki, D.J. & Ogston, A.S. (2013) Water and sediment transport of channel-flat systems in a mesotidal mudflat: Willapa Bay, Washington. *Continental Shelf Research*, 60, S111–S124.

Pernthaler, J., Glockner, F.O., Schonhuber, W. & Amann, R. (2001) Fluorescence in situ hybridization (FISH) with rRNA-targeted oligonucleotide probes. *Methods in Microbiology*, 30(30), 207–226.

Pfeffer, C., Larsen, S., Song, J., Dong, M.D., Besenbacher, F., Meyer, R.L. et al. (2012) Filamentous bacteria transport electrons over centimetre distances. *Nature*, 491, 218–221.

Plum-Jensen, L.E., Schramm, A. & Marshall, I.P.G. (2024) First single-strain enrichments of *Electrothrix* cable bacteria, description of *E. aestuarii* sp. nov. and *E. rattekaaiensis* sp. nov., and proposal of a cable bacteria taxonomy following the rules of the SeqCode. *Systematic and Applied Microbiology*, 47, 126487.

Quast, C., Pruesse, E., Yilmaz, P., Gerken, J., Schweer, T., Yarza, P. et al. (2013) The SILVA ribosomal RNA gene database project: improved data processing and web-based tools. *Nucleic Acids Research*, 41, D590–D596.

Risgaard-Petersen, N., Kristiansen, M., Frederiksen, R.B., Dittmer, A.L., Bjerg, J.T., Trojan, D. et al. (2015) Cable bacteria in freshwater sediments. *Applied and Environmental Microbiology*, 81, 6003–6011.

Sasada, R., Weinstein, M., Prem, A., Jin, M. & Bhasin, J. (2020) FIGARO: an efficient and objective tool for optimizing microbiome rRNA gene trimming parameters. *Journal of Biomolecular Techniques*, 31, S2.

Schauer, R., Risgaard-Petersen, N., Kjeldsen, K.U., Bjerg, J.J.T., Jorgensen, B.B., Schramm, A. et al. (2014) Succession of cable bacteria and electric currents in marine sediment. *The ISME Journal*, 8, 1314–1322.

Schindelin, J., Arganda-Carreras, I., Frise, E., Kaynig, V., Longair, M., Pietzsch, T. et al. (2012) Fiji: an open-source platform for biological-image analysis. *Nature Methods*, 9, 676–682.

Scholz, V.V., Martin, B.C., Meyer, R., Schramm, A., Fraser, M.W., Nielsen, L.P. et al. (2021) Cable bacteria at oxygen-releasing roots of aquatic plants: a widespread and diverse plant-microbe association. *New Phytologist*, 232, 2138–2151.

Scholz, V.V., Meckenstock, R.U., Nielsen, L.P. & Risgaard-Petersen, N. (2020) Cable bacteria reduce methane emissions from rice-vegetated soils. *Nature Communications*, 11, 1878.

Scilipoti, S., Koren, K., Risgaard-Petersen, N., Schramm, A. & Nielsen, L.P. (2021) Oxygen consumption of individual cable bacteria. *Science Advances*, 7, eabe1870.

Sereika, M., Petriglieri, F., Jensen, T.B.N., Sannikov, A., Hoppe, M., Nielsen, P.H. et al. (2023) Closed genomes uncover a saltwater species of *Electronema* and shed new light on the boundary between marine and freshwater cable bacteria. *The ISME Journal*, 17, 561–569.

Staley, J.T. & Gosink, J.J. (1999) Poles apart: biodiversity and biogeography of sea ice bacteria. *Annual Review of Microbiology*, 53, 189–215.

Strohl, W.R. & Larkin, J.M. (1978) Cell-division and trichome breakage in *Beggiatoa*. *Current Microbiology*, 1, 151–155.

Thorup, C., Petro, C., Boggild, A., Ebsen, T.S., Brokjaer, S., Nielsen, L.P. et al. (2021) How to grow your cable bacteria: establishment of a stable single-strain culture in sediment and proposal of *Candidatus Electronema aureum* GS. *Systematic and Applied Microbiology*, 44, 126236.

Trojan, D., Schreiber, L., Bjerg, J.T., Boggild, A., Yang, T.T., Kjeldsen, K.U. et al. (2016) A taxonomic framework for cable bacteria and proposal of the candidate genera *Electrothrix* and *Electronema*. *Systematic and Applied Microbiology*, 39, 297–306.

van der Veen, J.R., Valianti, S., van der Zant, H.S.J., Blanter, Y.M. & Meysman, F.J.R. (2024) A model analysis of centimeter-long electron transport in cable bacteria. *Physical Chemistry Chemical Physics*, 26, 3139–3151.

Vasquez-Cardenas, D., van de Vossenberg, J., Polerecky, L., Malkin, S.Y., Schauer, R., Hidalgo-Martinez, S. et al. (2015) Microbial carbon metabolism associated with electrogenic sulphur oxidation in coastal sediments. *The ISME Journal*, 9, 1966–1978.

Vellend, M. (2010) Conceptual synthesis in community ecology. *Quarterly Review of Biology*, 85, 183–206.

Yin, H., Aller, R.C., Zhu, Q.Z. & Aller, J.Y. (2021) The dynamics of cable bacteria colonization in surface sediments: a 2D view. *Scientific Reports*, 11, 7167.

**How to cite this article:** van Dijk, J.R., Geelhoed, J.S., Ley, P., Hidalgo-Martinez, S., Portillo-Estrada, M., Verbruggen, E. et al. (2024) Cable bacteria colonise new sediment environments through water column dispersal. *Environmental Microbiology*, 26(10), e16694. Available from: https://doi.org/10.1111/1462-2920.16694

## APPENDIX A

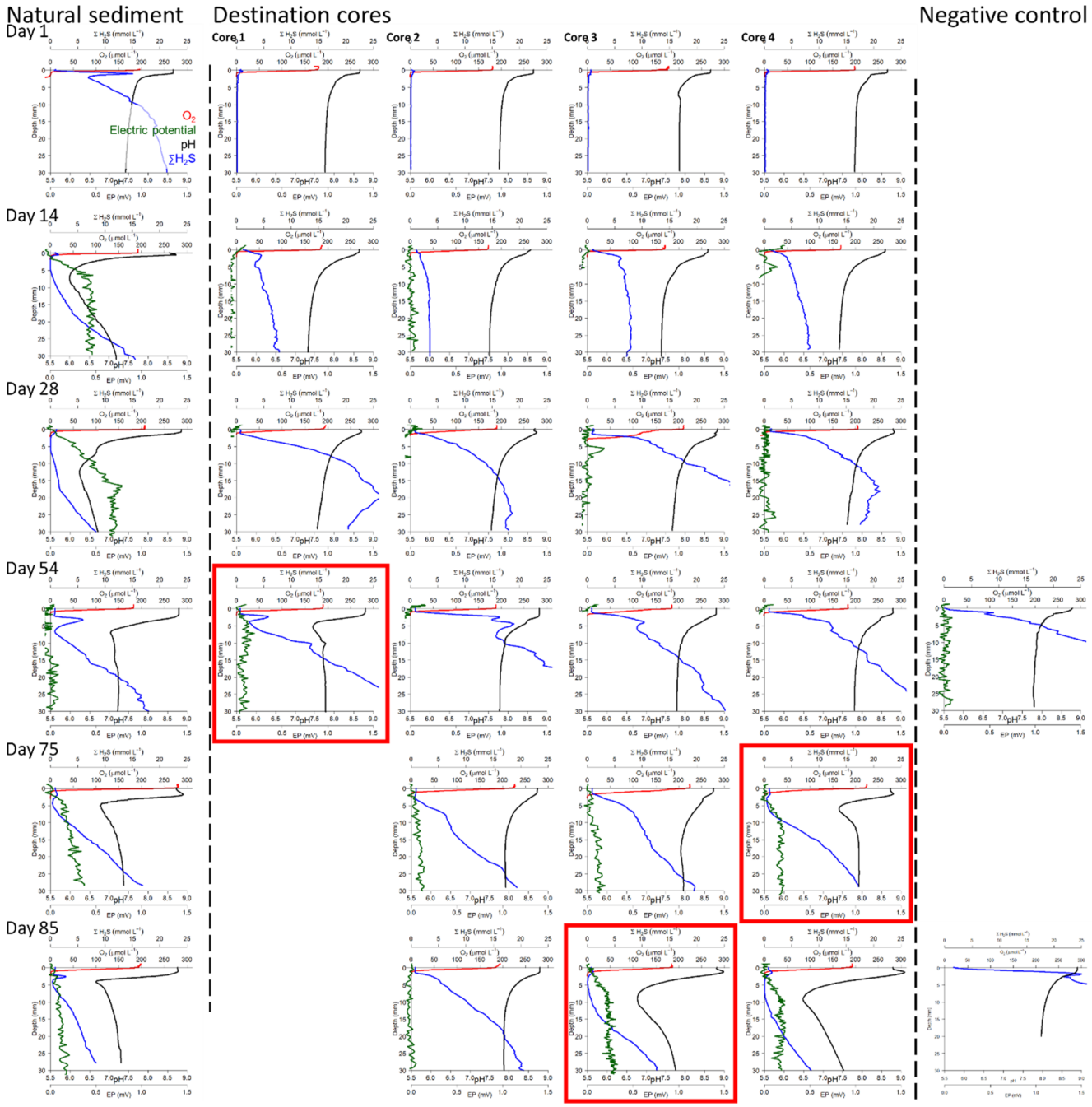


FIGURE A1 Microsensor profiles of the natural sediment, destination cores and negative controls throughout the experiment. The oxygen profile is plotted in red, the pH in black, the electric potential in green and the sum sulphide is calculated from the sulphide and pH profiles and is plotted in blue. The first sampling time when the characteristic fingerprint of cable bacteria activity in a destination core was detected in the profiles is marked with a red box. In DC2, based on the microsensor depth profiles, no cable bacteria activity was detected. However, FISH and amplicon sequencing showed a low abundance of cable bacteria. The plots show a duplicate microsensor depth profile as a dotted line.

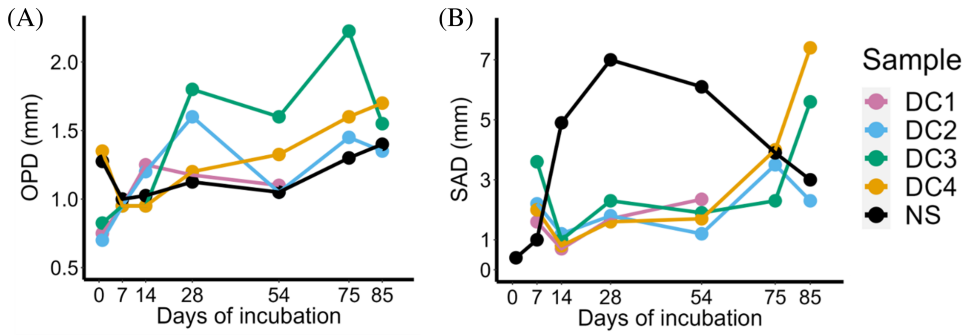


**FIGURE A2** Temporal evolution of the (A) oxygen penetration depth and (B) sulphide appearance depth obtained by microsensor profiling in the natural sediment (NS) and the destination cores (DC). The values shown (dots) are calculated from the individual profiles and the line drawn through the average values. For the natural sediment, multiple spots were profiled, resulting in four datapoints, as opposed to two datapoints for the destination cores.